

Reactions of Platinum–Carbene Clusters Pt_nCH_2^+ ($n = 1-5$) with O_2 , CH_4 , NH_3 , and H_2O : Coupling Processes versus Carbide Formation[†]

Konrad Koszinowski, Detlef Schröder, and Helmut Schwarz*

Institut für Chemie der Technischen Universität Berlin, Strasse des 17. Juni 135, D-10623 Berlin, Germany

Received April 15, 2003

The gas-phase reactions of the platinum–carbene clusters Pt_nCH_2^+ ($n = 2-5$) with the substrates O_2 , CH_4 , NH_3 , and H_2O have been investigated by FT-ICR mass spectrometry and compared with previous results for the mononuclear homologue PtCH_2^+ . The ion–molecule reactions of the clusters Pt_nCH_2^+ with O_2 and CH_4 are similar to the corresponding processes observed for PtCH_2^+ . In contrast, a surprising difference evolves in the reactions with NH_3 and H_2O . Whereas PtCH_2^+ mediates carbon–heteroatom bond formation as an attractive way toward methane functionalization, the homologous clusters fail in this regard and exclusively yield the carbide complexes $\text{Pt}_n\text{C}^+\cdot\text{NH}_3$ and $\text{Pt}_n\text{C}^+\cdot\text{H}_2\text{O}$, respectively. The differences in reactivities have been analyzed further by means of kinetic isotope effects, H/D-exchange reactions, and energy-dependent collision-induced dissociations of Pt_nCH_2^+ . Essentially, the higher stabilities of the platinum–carbide clusters Pt_nC^+ compared to PtC^+ cause the change in reactivity. This conclusion is confirmed by the reactions of independently generated clusters Pt_nC^+ ($n = 1-5$) with O_2 , CH_4 , NH_3 , and H_2O . The results underline the importance of carbide structures in these gas-phase reactions, thereby resembling catalyst deactivation by soot formation on heterogeneous platinum catalysts.

Introduction

The limitation of petrochemical feedstocks has provoked tremendous interest in the usage of natural gas resources as raw materials for chemical industry. Functionalization of methane as the most abundant alkane has received particular attention, and its conversion to methanol remains one of the great challenges for catalysis to date.^{1–3} Like C–H bond activation in general, methane functionalization is severely hampered by the unfavorable order of reactivities between the reactant and products: whereas methane is relatively inert and exhibits strong C–H bonds ($D_0(\text{CH}_3\text{–H}) = 433 \text{ kJ mol}^{-1}$),⁴ functionalized products are much more reactive and, thus, prone to overoxidation, unless very selective activation of CH_4 is achieved.

One of the most promising approaches toward the functionalization of methane relies on transition-metal chemistry.^{5,6} Among the transition metals used for catalytic C–H bond activation, platinum is of particular importance, as far as methane conversion is concerned. Recently, Pt(II) salts have been shown to catalyze the selective oxidation of CH_4 under homogeneous conditions,⁷ and both the Degussa and Andrussov processes for the

large-scale synthesis of hydrogen cyanide (reactions 1 and 2) are well-established paths of methane refinement mediated by heterogeneous platinum catalysts.^{8–11}



The rational development of improved or new catalytic reactions for the functionalization of methane requires detailed mechanistic insight into the processes already known. However, the complexity of these processes, especially those of heterogeneous catalysis such as reactions 1 and 2, often makes an in situ characterization of the elementary reactions involved nearly impossible. It is therefore a common strategy to use model systems which still feature the essential characteristics of the real catalytic processes but simultaneously significantly reduce their intricacy and, thus, enable thorough mechanistic elucidation. The most drastic simplification conceivable focuses only on the intrinsic reactivity of the catalytically active transition metal and excludes all other constituents of the real system, such as ligands, counterions, lattices, or solvents. Such a model is realized by gaseous transition-metal ions whose chemical behavior can be investigated in depth by advanced mass spectrometric methods.¹²

[†] Dedicated to Professor Werner Schroth, Halle, on the occasion of his 75th birthday.

* Corresponding author.

(1) *Chem. Eng. News* **1993** (May 31), 71, 27.
 (2) Muehlhofer, M.; Strassner, T.; Herrmann, W. A. *Angew. Chem.* **2002**, 114, 1817; *Angew. Chem., Int. Ed.* **2002**, 41, 1745.
 (3) Fokin, A. A.; Schreiner, P. R. *Chem. Rev.* **2002**, 102, 1551.
 (4) Litorja, M.; Ruscic, B. *J. Chem. Phys.* **1997**, 107, 9852.
 (5) Litorja, M.; Bercaw, J. E. *Nature* **2002**, 417, 507.
 (6) Schwarz, H.; Schröder, D. *Pure Appl. Chem.* **2000**, 72, 2319.
 (7) Periana, R. A.; Taube, D. J.; Gamble, S.; Taube, H.; Satoh, T.; Fujii, H. *Science* **1998**, 280, 560.

(8) Hasenberg, D.; Schmidt, L. D. *J. Catal.* **1986**, 97, 156.
 (9) Hasenberg, D.; Schmidt, L. D. *J. Catal.* **1987**, 104, 441.
 (10) Waletzko, N.; Schmidt, L. D. *AIChE J.* **1988**, 34, 1146.
 (11) Bockholt, A.; Harding, I. S.; Nix, R. M. *J. Chem. Soc., Faraday Trans.* **1997**, 93, 3869.
 (12) Eller, K.; Schwarz, H. *Chem. Rev.* **1991**, 91, 1121.

With regard to the Degussa process, our group has recently presented a gas-phase model based on cationic platinum atoms Pt^+ that indeed mirrors the reactivity of the heterogeneous catalyst.^{13,14} Remarkably, platinum's capability to mediate C–N bond formation was found to be superior to that of several other late-transition-metal ions studied. The investigations further revealed that cationic platinum carbene, PtCH_2^+ , which is readily produced by dehydrogenation of CH_4 (reaction 3 with $n = 1$),¹⁵ is a key intermediate on the path toward



C–N bond coupling. The reactions of PtCH_2^+ with other small nucleophiles, such as water, phosphine, and hydrogen sulfide, also bring about the formation of carbon–heteroatom bonds;¹⁶ these processes appear to constitute a fairly general model of methane functionalization in the gas phase.

A straightforward modification replaces atomic Pt^+ by small clusters Pt_n^+ . In comparison with single atoms, transition-metal clusters such as Pt_n^+ are generally thought to resemble the bulk catalyst more closely because of the higher degree of association.¹⁷ In fact, Pt_n^+ clusters have been shown to dehydrogenate CH_4 according to reaction 3.^{17,18} However, as already emphasized above, methane conversion requires both activation of CH_4 and coupling of the reactive intermediate with an appropriate substrate. In the present work, we focus on the second step and investigate the gas-phase reactivities of the cluster species Pt_nCH_2^+ and Pt_nC^+ ($n \leq 5$), using Fourier transform ion-cyclotron resonance (FT-ICR) mass spectrometry. Also, the carbide clusters Pt_nC^+ are included in this study because these are accessible by interaction of Pt_n^+ with CH_4 as well and they might possibly also undergo coupling reactions. Moreover, the carbide clusters prove useful for a better understanding of the reactivities of the Pt_nCH_2^+ clusters.

As a probe for the chemical behavior of Pt_nCH_2^+ and Pt_nC^+ , their reactivities toward dioxygen, methane, ammonia, and water are considered. NH_3 and H_2O are typical nucleophiles appropriate as examples in a study of carbon–heteroatom coupling. CH_4 , on the other hand, is an element hydride as well but lacks nucleophilicity, such that a comparison between the reactivities of the different neutral reactants promises to reveal the influence of the substrates' electronic properties on the course of reaction. Reaction of the clusters with O_2 , the most versatile oxidant, provides another potential route for methane functionalization. Any proper interpretation of the experimental results crucially depends on structural assignments for the products observed, as achieved by isotopic labeling and collision-induced dis-

Table 1. Bimolecular Rate Constants k and Efficiencies φ for the Reactions of Pt_nCH_2^+ with NH_3 , H_2O , CH_4 , and O_2 , Respectively

reaction	eq no.	n	$k/\text{cm}^3\text{s}^{-1}$	$\varphi = k/k_c^a$
$\text{PtCH}_2^+ + \text{NH}_3 \rightarrow \text{NH}_4^+ + \text{PtCH}$	4		$3.1 \times 10^{-11}{}^b$	0.015
$\text{PtCH}_2^+ + \text{NH}_3 \rightarrow \text{CH}_2\text{NH}_2^+ + \text{PtH}$	5		$4.3 \times 10^{-10}{}^b$	0.21
$\text{Pt}_n\text{CH}_2^+ + \text{NH}_3 \rightarrow [\text{Pt}_n\text{C,H}_3\text{,N}]^+ + \text{H}_2$	6	1	$1.6 \times 10^{-10}{}^b$	0.089
	2		9.7×10^{-10}	0.49
	3		9.6×10^{-10}	0.48
	4		1.7×10^{-9}	0.86
	5		1.2×10^{-9}	0.61
$\text{PtCH}_2^+ + \text{H}_2\text{O} \rightarrow \text{PtCO}^+ + 2\text{H}_2$	10		$2 \times 10^{-13}{}^c$	8×10^{-5}
$\text{Pt}_n\text{CH}_2^+ + \text{H}_2\text{O} \rightarrow [\text{Pt}_n\text{C,H}_2\text{,O}]^+ + \text{H}_2$	11	1	$4 \times 10^{-12}{}^c$	2×10^{-3}
	2		$\leq 8 \times 10^{-14}$	$\leq 3 \times 10^{-5}$
	3		1.1×10^{-11}	5×10^{-3}
	4		9.4×10^{-10}	0.41
	5		1.0×10^{-10}	0.044
$\text{Pt}_n\text{CH}_2^+ + \text{CH}_4 \rightarrow [\text{Pt}_n\text{C}_2\text{,H}_4]^+ + \text{H}_2$	14	1	$2 \times 10^{-11}{}^b$	0.02
	2–4		$\leq 2 \times 10^{-12}$	$\leq 2 \times 10^{-3}$
	5		2.5×10^{-10}	0.26
	17		$7 \times 10^{-12}{}^d$	0.012
	18	1	$1.6 \times 10^{-11}{}^d$	0.028
$\text{Pt}_n\text{CH}_2^+ + \text{O}_2 \rightarrow \text{PtO}^+ + \text{CH}_2\text{O}$ $\text{Pt}_n\text{CH}_2^+ + \text{O}_2 \rightarrow \text{Pt}_n^+ + [\text{C,H}_2\text{,O}_2]$	2		$\leq 2 \times 10^{-13}$	$\leq 4 \times 10^{-4}$
	3		4.5×10^{-12}	8×10^{-3}
	4		9.0×10^{-11}	0.17
	5		1.3×10^{-10}	0.25

^a Collision rates k_c calculated according to capture theory (Su, T. J. *Chem. Phys.* **1988**, *89*, 4102, 5355). ^b Taken from ref 14. ^c Taken from ref 16. ^d Taken from ref 23.

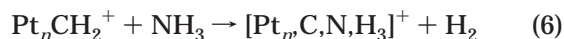
sociation (CID) experiments. The same techniques are also used to gain insight into the potential-energy surfaces of the systems $\text{Pt}_n^+/\text{CH}_4$.

As mentioned already, the reactions of the mononuclear PtCH_2^+ relevant in the present context have been reported previously.^{13,14,16} Recently also the reactivities of the clusters Pt_nCH_2^+ ($n \leq 5$) toward CH_4 have been described¹⁹ and we briefly reported on their reactions with NH_3 .²⁰ For comparison, these data are included in the present study.

Results and Discussion

The first section deals with the reactivities of platinum–carbene clusters Pt_nCH_2 ($n = 1–5$) toward NH_3 , H_2O , CH_4 , and O_2 . Moreover, H/D exchange reactions, kinetic isotope effects (KIEs), and CID processes are investigated. The second section focuses on the corresponding reactions of platinum–carbide clusters Pt_nC , $n = 1–5$.

Pt_nCH_2^+ . (a) Reactions with Ammonia. Reaction of PtCH_2^+ with NH_3 occurs efficiently (Table 1), yielding three different products (reactions 4–6 with $n = 1$).¹³



Whereas reaction 4, a simple proton transfer from the platinum carbene to NH_3 , accounts for only 5% of the total product formation, reaction 5 constitutes the main product channel (70% branching ratio, br) and unambiguously proves C–N bond coupling. Interpretation of

(19) Koszinowski, K.; Schröder, D.; Schwarz, H. *J. Phys. Chem. A* **2003**, *107*, 4999.

(20) Koszinowski, K.; Schröder, D.; Schwarz, H. *J. Am. Chem. Soc.* **2003**, *125*, 3676.

(13) (a) Aschi, M.; Brönstrup, M.; Diefenbach, M.; Harvey, J. N.; Schröder, D.; Schwarz, H. *Angew. Chem.* **1998**, *110*, 858; *Angew. Chem., Int. Ed.* **1998**, *37*, 829. (b) Recent experiments find $D_0(\text{Pt}^+-\text{NH}_3) = 274 \pm 12$ kJ mol⁻¹; see: Liyanage, R.; Styles, M. L.; O'Hair, R. A. J.; Armentrout, P. B. *Int. J. Mass Spectrom.* **2003**, *227*, 47.

(14) Diefenbach, M.; Brönstrup, M.; Aschi, M.; Schröder, D.; Schwarz, H. *J. Am. Chem. Soc.* **1999**, *121*, 10614.

(15) Irakura, K. K.; Beauchamp, J. L. *J. Phys. Chem.* **1991**, *95*, 8344.

(16) Brönstrup, M.; Schröder, D.; Schwarz, H. *Organometallics* **1999**, *18*, 1939.

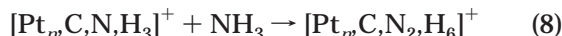
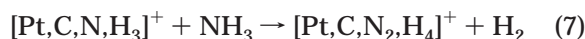
(17) Kaldor, A.; Cox, D. M. *Pure Appl. Chem.* **1990**, *62*, 79.

(18) Achatz, U.; Berg, C.; Joos, S.; Fox, B. S.; Beyer, M. K.; Niedner-Schatteberg, G.; Bondyby, V. E. *Chem. Phys. Lett.* **2000**, *320*, 53.

reaction 6 (25% br for $n = 1$) is less straightforward because a structural assignment of the ionic product needs to be achieved at first.

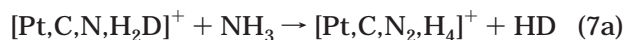
For the homologous clusters Pt_nCH_2^+ ($n = 2-5$) only reaction 6 is observed (Table 1). The absence of reactions 4 and 5 for the cluster ions is no surprise, because their occurrence in the case of PtCH_2^+ reflects the high ionization energy of atomic Pt, $\text{IE}(\text{Pt}) = 9.0 \text{ eV}$,²¹ which disfavors location of the positive charge at the metal-containing product. For the clusters, however, the larger metal core can more easily accommodate a positive charge (compare $\text{IE}(\text{Pt}_2) = 8.68 \pm 0.02 \text{ eV}$)²² such that reaction 6 is expected to gain in importance, as observed experimentally.

Consideration of the consecutive reactions of $[\text{Pt}_m\text{C}_n\text{N}_3\text{H}_3]^+$ provides further insight into the structures of the product ions. The corresponding $[\text{Pt}_m\text{C}_n\text{N}_3\text{H}_3]^+$ species derived from mononuclear Pt^+ reacts with another NH_3 molecule under dehydrogenation (reaction 7).^{13,14} In contrast, the cluster ions $[\text{Pt}_m\text{C}_n\text{N}_3\text{H}_3]^+$ ($n = 2-5$) do not activate ammonia but simply form adducts (reaction 8; efficiencies up to 8% for $n = 5$). Presumably, these processes are assisted by termolecular stabilization. The different behaviors ob-



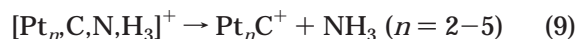
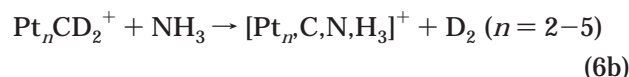
served for $[\text{Pt}_m\text{C}_n\text{N}_3\text{H}_3]^+$ on one hand and for the clusters $[\text{Pt}_m\text{C}_n\text{N}_3\text{H}_3]^+$ on the other might indicate the presence of different ion structures. DFT calculations predict $[\text{Pt}_m\text{C}_n\text{N}_3\text{H}_3]^+$ to correspond to an aminocarbene, $\text{PtC}(\text{H})\text{NH}_2^+$.¹⁴ In the consecutive reaction with NH_3 (reaction 7), the hydrogen atom bound to carbon is replaced with an amino group, thus generating the diaminocarbene $\text{PtC}(\text{NH}_2)_2^+$ as the product.¹⁴ No theoretical results are available for the corresponding cluster ions. In fact, the presence of additional Pt atoms tremendously complicates the theoretical description of the system so that one might doubt that current ab initio techniques could handle this situation. Hence, for the time being we have to rely on experiment in the further discussion.

A valuable tool for structural elucidation in mass spectrometry is isotopic labeling. With respect to the problem under investigation, usage of deuterated carbenes Pt_nCD_2^+ is particularly helpful. As shown previously, PtCD_2^+ loses HD in the process analogous to reaction 6 for $n = 1$ (reaction 6a). In the consecutive reaction 7a, again loss of HD occurs.¹³ Both observations are in full accordance with the structural assignments provided by theory.

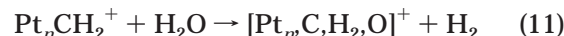


In marked contrast, the deuterated carbenes of platinum cluster ions exclusively lose D_2 upon reaction with NH_3 (reaction 6b with $n = 2-5$). This is clear evidence that the carbenes derived from platinum clusters behave

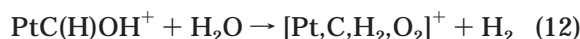
differently from that containing only a single metal center. Specifically, aminocarbene structures appear unlikely for $[\text{Pt}_m\text{C}_n\text{N}_3\text{H}_3]^+$ ($n = 2-5$) because either selective loss of HD or H/D scrambling is expected, but not exclusive elimination of D_2 . Instead, the labeling experiments suggest that the NH_3 molecule remains intact and forms an adduct with a platinum–carbide moiety, i.e., $\text{Pt}_m\text{C}^+\cdot\text{NH}_3$. The same conclusion can be inferred from collision-induced dissociation of $[\text{Pt}_m\text{C}_n\text{N}_3\text{H}_3]^+$, which yields Pt_mC^+ as the only ionic products at variable collisional energies (reaction 9). In contrast, CID of the aminocarbene $\text{PtC}(\text{H})\text{NH}_2^+$ gives a mixture of $[\text{Pt}_m\text{C}_n\text{N}_3\text{H}_3]^+$, CH_2NH_2^+ , and Pt^+ as ionic fragments;¹³ this, again, demonstrates the dissimilarity between the system $\text{PtCH}_2^+/\text{NH}_3$ and the formally analogous platinum-cluster ions.



(b) Reactions with Water. Upon changing the substrate from ammonia to water, a drastic decrease in reactivity was observed for PtCH_2^+ (Table 1). Apparently, the lower nucleophilicity of H_2O renders an attack at the electrophilic carbene less favorable than in the case of NH_3 . The different electronic properties of H_2O are also mirrored in a change of product channel (reactions 10 and 11 with $n = 1$).¹⁶ Whereas reaction



10 only represents a minor process (5% br), reaction 11 is the main channel, yielding the hydroxycarbene $\text{PtC}(\text{H})\text{OH}^+$ for $n = 1$ in analogy to the corresponding reaction with NH_3 .¹⁶ The two other processes observed for the system $\text{PtCH}_2^+/\text{NH}_3$, reactions 4 and 5, do not have counterparts for the case of H_2O . Most likely, the lower basicity of H_2O and the increased electronegativity of oxygen result in an unfavorable thermochemistry with respect to charge transfer away from the metal center. Similarly to $\text{PtC}(\text{H})\text{NH}_2^+$, $\text{PtC}(\text{H})\text{OH}^+$ undergoes an efficient consecutive reaction with a further substrate molecule (reaction 12).¹⁶

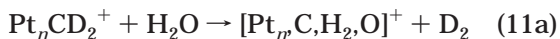


Let us now turn to the reactions of the corresponding clusters. Whereas Pt_2CH_2^+ does not react with H_2O , the larger clusters Pt_nCH_2^+ ($n = 3-5$) afford dehydrogenation (reaction 11). As seen above, this finding alone is not sufficient to discriminate between the two reactivity patterns identified so far. However, the fact that no measurable consecutive reactions occurred at the pressures applied is a first indication that the clusters behave differently from PtCH_2^+ . Of course, simple adducts $[\text{Pt}_m\text{C}_n\text{H}_2\text{O}]^+\cdot\text{H}_2\text{O}$ may be formed by termolecular stabilization at higher pressures, but FT-ICR mass spectrometry is not the method of choice to study such processes because the operating pressures are very low. Again, deuterium labeling (reaction 11a), combined

(21) <http://webbook.nist.gov/chemistry/>.

(22) Taylor, S.; Lemire, G. W.; Hamrick, Y. M.; Fu, Z.; Morse, M. D. *J. Chem. Phys.* **1988**, *89*, 5517.

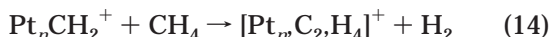
with CID experiments (reaction 13), provide more specific information. Upon reaction of Pt_nCD_2^+ , $n = 3-5$,



with H_2O , D_2 is lost exclusively (reaction 11a). This result is in marked contrast to elimination of HD from PtCD_2^+ upon reaction with H_2O ,¹⁶ whereas it parallels the clusters' reactivities toward NH_3 . Moreover, CID of the $[\text{Pt}_n\text{C,H}_2\text{O}]^+$ products solely gives Pt_nC^+ as an ionic fragment (reaction 13). Much like in the case of ammonia, these results thus indicate the formation of mere adducts between platinum-carbide clusters and H_2O : i.e., $\text{Pt}_n\text{C}^+\cdot\text{H}_2\text{O}$.

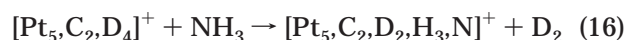
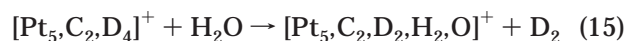
In summary, all experimental results agree that, unlike mononuclear PtCH_2^+ , the oligonuclear platinum-carbene ions do not effect carbon-heteroatom bond formation upon reaction with the nucleophiles ammonia and water. Rather, the substrates appear to simply replace both hydrogen atoms of the carbene fragment, resulting in ion-molecule complexes of a carbide cluster Pt_nC^+ and the substrate. The large efficiencies observed in the reactions with NH_3 for all cluster sizes studied (Table 1) imply that the encounter of both reactants releases sufficient energy to easily overcome all barriers involved en route to the products. In contrast, the lower basicity of water reduces the interaction energy such that differences in the reactivities of different cluster sizes become apparent. Whereas no reaction occurs for the carbene derived from the dinuclear cluster Pt_2CH_2^+ , those with $n = 3$ and $n = 5$ react with moderate efficiency and that with $n = 4$ with high efficiency. This order is supposed to inversely correlate with the stabilities of the carbene-cluster sizes. Interestingly, formation of Pt_4CH_2^+ from Pt_4^+ and CH_4 according to reaction 3 was found to be anomalously slow, thus being in agreement with the enhanced reactivity of this species toward H_2O (see below).^{18,19}

(c) Reactions with Methane. The third element hydride included in the present study, methane, differs from its counterparts NH_3 and H_2O in its lack of a lone electron pair and the resulting absence of nucleophilicity. As reported previously, only PtCH_2^+ and Pt_5CH_2^+ induce dehydrogenation of a further CH_4 molecule (reaction 14 with $n = 1, 5$) (Table 1).¹⁹ With regard to

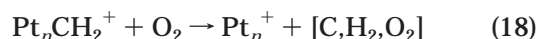


the observations presented above, it is not unexpected that the behavior of PtCH_2^+ differs from that of the analogous clusters Pt_nCH_2^+ ($n = 2-4$). Occurrence of reaction 14 for $n = 5$ can be attributed to the enlarged metal core for this cluster size, which might accommodate two CH_2 fragments.¹⁹ Accordingly, the two carbon moieties are thought to remain separated from each other, in contrast to the situation for $n = 1$, where both methylene fragments combine to give an ethylene molecule bound to Pt^+ .¹⁴ To further probe the structure assigned to $[\text{Pt}_5\text{C}_2\text{H}_4]^+$, the ion was subjected to CID, which affords single and double dehydrogenation but no losses of C_1 or C_2 fragments. If both methylene fragments combine to yield an ethylene molecule complexed to the Pt_5^+ core, facile ligand exchange (ex) would

be expected upon exposure of isotopically labeled $[\text{Pt}_5\text{C}_2\text{D}_4]^+$ to C_2H_4 ($k_{\text{ex}} \approx 1/2k_c$, $k_c = \text{collision rate}$). Because such exchange was not observed above the noise level ($k_{\text{ex}} \leq 1/4k_c$), we tentatively discard a $\text{Pt}_5^+\cdot\text{C}_2\text{X}_4$ ($\text{X} = \text{H}, \text{D}$) structure. Regarding its reactivity, $[\text{Pt}_5\text{C}_2\text{D}_4]^+$ adds H_2O concomitant with loss of D_2 (reaction 15); an analogous process occurs in the presence of NH_3 (reaction 16). Accordingly, formal addition of a further CH_2 fragment to Pt_5CH_2^+ does not seem to significantly change its chemical behavior.



(d) Reactions with Dioxxygen. Another potential way to methane functionalization relies on reactions with oxygen. PtCH_2^+ was found to react rather slowly with O_2 (Table 1), yielding PtO^+ (30% br) and Pt^+ (70% br) as ionic products according to reactions 17 and 18 with $n = 1$.²³ Whereas the formation of formaldehyde



in reaction 17 can safely be inferred on thermochemical grounds, the nature of the neutral product formed in reaction 18 is less clear. For the mononuclear system, elaborate theoretical studies indicate that formation of HCOOH , $\text{CO}/\text{H}_2\text{O}$, or CO_2/H_2 is feasible and that most likely a mixture of these species is generated.²⁴ Taking into account the consecutive reactions occurring for Pt^+ and PtO^+ in the presence of CH_4 and O_2 , an extended catalytic cycle for methane oxidation evolves. Note, however, that the only moderate selectivities of the different processes somewhat impair its attractiveness.^{23,24}

With respect to the clusters Pt_nCH_2^+ , no reactivity is observed for $n = 2$, whereas reaction 18 takes place with increasing efficiencies for the larger clusters. In the case of Pt_5CH_2^+ , small amounts of Pt_5O^+ are observed as well, which might point to the occurrence of a process analogous to reaction 17 as a minor channel for $n = 5$. This assignment is uncertain, however, because the inevitable presence of traces of background water in the high-vacuum system also leads to formation of $\text{Pt}_5\text{C}^+\cdot\text{H}_2\text{O}$ (reaction 11), which, in analogy to $\text{Pt}_4\text{C}^+\cdot\text{H}_2\text{O}$, in turn might afford Pt_5O^+ under exposure of O_2 (see below). As for the $\text{PtCH}_2^+/\text{O}_2$ system, the structure of the neutral product of reaction 18 cannot be inferred from experiment; again, formation of HCOOH , $\text{CO}/\text{H}_2\text{O}$, or CO_2/H_2 appears reasonable. Obviously, the reactions of the clusters Pt_nCH_2^+ ($n = 3-5$) with O_2 mediate carbon-oxygen bond formation, in contrast to the reactions with H_2O . Whereas the Pt_nCH_2^+ ions only lose their hydrogen atoms in the latter processes, it is no surprise that the reactions with O_2 also involve the carbon atom: combination with the two hydrogen atoms merely saturates two valences of O_2 and, thus, would

(23) Wesendrup, R.; Schröder, D.; Schwarz, H. *Angew. Chem.* **1994**, *106*, 1232; *Angew. Chem., Int. Ed. Engl.* **1994**, *33*, 1174.

(24) Pavlov, M.; Blomberg, M. R. A.; Siegbahn, P. E. M.; Wesendrup, R.; Heinemann, C.; Schwarz, H. *J. Phys. Chem. A* **1997**, *101*, 1567.

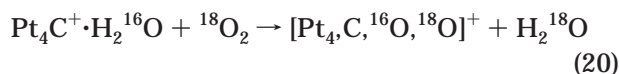
lead to thermochemically unfavorable products such as H_2O_2 and $\text{H}_2\text{O}/\text{O}$. In contrast, participation of carbon allows reduction of both oxygen atoms to their most stable oxidation state, $-II$, thereby providing a strong driving force for the overall reaction.

The distinct reactivities of the platinum–carbene clusters toward O_2 prompted us to also investigate the corresponding reactions of $\text{Pt}_n\text{C}^+\cdot\text{NH}_3$ and $\text{Pt}_n\text{C}^+\cdot\text{H}_2\text{O}$. However, as the production of these ions requires leaking in of NH_3 and H_2O , respectively, into the ICR cell, the presence of these substrates besides that of O_2 significantly obscures the kinetic analysis of the reactions of interest. We therefore refrain from deriving quantitative data for these processes and only focus on the cluster size $n = 4$. Upon reaction of $\text{Pt}_4\text{C}^+\cdot\text{NH}_3$ with O_2 , $[\text{Pt}_4\text{H}_2\text{N}]^+$ is formed as the primary product (reaction 19), which then gives rise to a plethora of consecu-



tive reactions (inter alia yielding $[\text{Pt}_4\text{H}_2\text{N}]^+$ and $[\text{Pt}_4\text{H}_2\text{N},\text{O}]^+$, whose origin is uncertain). The neutral product of reaction 19 has the same formula as that of reaction 18 and may have the same structural possibilities. With respect to the ionic product, assumption of an imine species, that is, Pt_4NH^+ , appears reasonable. In any case, the reaction is clear evidence for oxidation of NH_3 . As this process certainly requires surpassing of considerable barriers, its occurrence implies the availability of significant amounts of energy during the course of the reaction. While loss of NH_3 concomitant with formation of CO_2 appears as a viable alternative process from a thermochemical point of view, this particular reaction does not occur in the experiment. The very reactivity observed indicates a strong binding between NH_3 and the cluster core. Lacking other information, the bond-dissociation energy of the mono-nuclear system, $D_0(\text{Pt}^+-\text{NH}_3) = 310 \text{ kJ mol}^{-1}$, as predicted by DFT calculations,¹³ may be used for comparison. The presence of more than a single metal center in the corresponding clusters is thought to further increase the interaction energy between NH_3 and the cluster core and may also help to reduce the barriers associated with NH_3 activation.

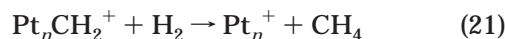
Reaction of $\text{Pt}_4\text{C}^+\cdot\text{H}_2\text{O}$ with O_2 yields $[\text{Pt}_4\text{C},\text{O}_2]^+$ as the primary product (reaction 20). Pt_4O^+ and Pt_4^+ were



observed as consecutive products, but their origin cannot be inferred unambiguously. Reaction 20 formally corresponds to a substitution of H_2O for O_2 . However, the isotopic labeling applied proves the activation of the water ligand in the course of the reaction, which requires extensive bond rearrangements. In contrast to reaction 19, only H_2O instead of $[\text{C},\text{H}_2,\text{O}_2]$ is lost. If one assumes comparable pathways for both reactions, $[\text{Pt}_4\text{C},\text{O}_2]^+$ should correspond to a platinum–oxide cluster ligated by one CO molecule. Apparently, the process involving $\text{Pt}_4\text{C}^+\cdot\text{H}_2\text{O}$ does not release sufficient energy to expel the CO ligand, whereas such an elimination is possible for the $\text{Pt}_4\text{C}^+\cdot\text{NH}_3/\text{O}_2$ system.

(e) Reactions with Dihydrogen. Returning to our initial subject, the reactivities of platinum–carbene

clusters themselves, also their chemical behavior toward hydrogen is of interest. Formation of methane upon reaction with H_2 , the reverse process of carbene generation according to reaction 3, has been observed for $n = 1, 4$ (reaction 21), which allows determination of the



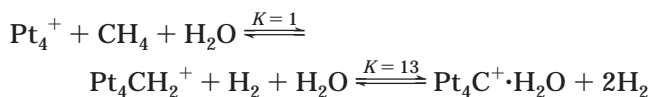
thermodynamics involved.^{19,24} Occurrence of reaction 21 for $n = 4$ implies that this carbene is less stable than those of the other cluster sizes studied, which well fits with the higher reactivity toward H_2O found for Pt_4CH_2^+ .

In the course of H/D exchange experiments (see below), the inevitable presence of background water led to formation of $\text{Pt}_4\text{C}^+\cdot\text{H}_2\text{O}$, which was found to further react with D_2 (reaction 22). Obviously, this process is



the reverse of reaction 11a. The ratio of rate constants for forward and backward reactions corresponds to the equilibrium constant, $K = k(11a)/k(22)$, which is further related to the free reaction enthalpy, $\Delta_r G^\circ_{298\text{K}} = -RT \ln K$. For the unlabeled case, i.e., reaction 11 and its reverse, one derives $K = 13 \pm 9$ and, thus, $\Delta_r G^\circ_{298\text{K}} = -6 \pm 3 \text{ kJ mol}^{-1}$. Hence, the thermodynamic equilibria connecting $\text{Pt}_4^+/\text{CH}_4/\text{H}_2\text{O}$, $\text{Pt}_4\text{CH}_2^+/\text{H}_2/\text{H}_2\text{O}$, and $\text{Pt}_4\text{C}^+\cdot\text{H}_2\text{O}/2 \text{ H}_2$ now are fully established (Scheme 1).¹⁹ In the case of the other clusters studied, the higher stability of the platinum–carbene species shifts the first equilibrium to the right (more efficient activation of methane), whereas the second one is shifted to the left (no reaction with dihydrogen).

Scheme 1



Usage of D_2 , rather than H_2 , enables monitoring of H/D exchange processes. Careful kinetic analysis should reveal the ratio of direct and stepwise substitution of H_2 for D_2 as a function of cluster size. In addition to reaction 21 observed for $n = 1, 4$, the following H/D exchange reactions may take place:

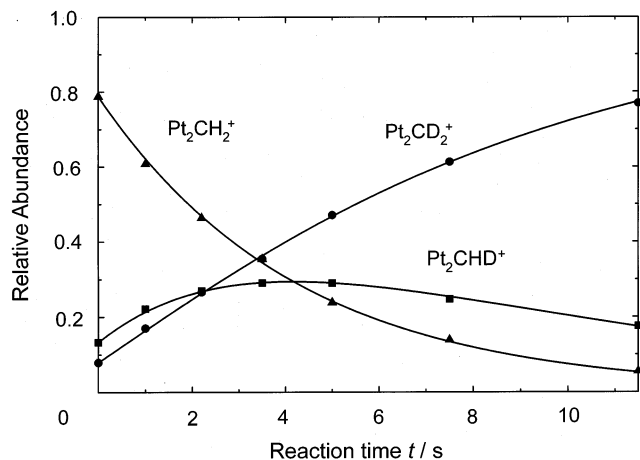
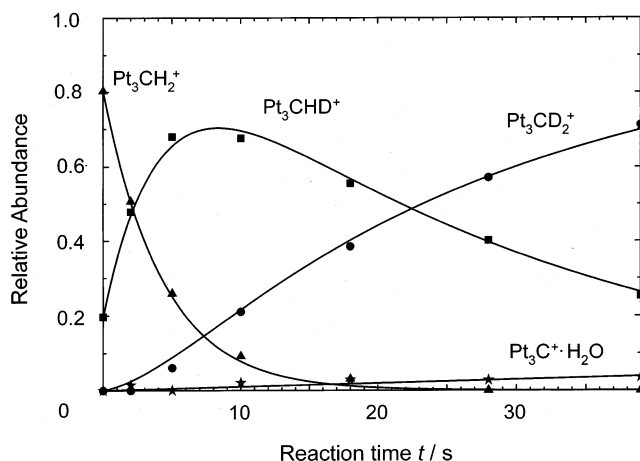


Reactions 23a and 23b constitute a stepwise exchange, whereas reaction 23c corresponds to direct substitution of H_2 for D_2 . As these processes involve either identical reactant or product ions, the determination of separate rate constants requires modeling according to the kinetic scheme defined by reactions 23a–c and reaction 21 for $n = 1, 4$. All sets of rate constants which give acceptable fits are acknowledged for the specification of their reliabilities (Table 2). For Pt_nCH_2^+ ($n = 3-5$), the interfering reactions with background water (see above) also have to be taken into account. Although the resulting complexity of the kinetic schemes limits the

Table 2. Bimolecular Rate Constants k for H/D Exchange Reactions of Pt_nCH_2^+ (Reactions 23a–c)

reacn	eq no.	$k/10^{-10} \text{ cm}^3 \text{ s}^{-1a}$				
		$n = 1$	$n = 2$	$n = 3$	$n = 4$	$n = 5$
$\text{Pt}_n\text{CH}_2^+ + \text{D}_2 \rightarrow \text{Pt}_n\text{CHD}^+ + \text{HD}$	23a	2.5 ± 0.3	2.1 ± 0.4	3.3 ± 0.4	4.1 ± 0.9	2.3 ± 0.8
$\text{Pt}_n\text{CHD}^+ + \text{D}_2 \rightarrow \text{Pt}_n\text{CD}_2^+ + \text{HD}$	23b	2.4 ± 0.5	2.1 ± 0.5	5.3 ± 0.5	9 ± 5	b
$\text{Pt}_n\text{CH}_2^+ + \text{D}_2 \rightarrow \text{Pt}_n\text{CD}_2^+ + \text{H}_2$	23c	1.1 ± 0.3	1.1 ± 0.4	< 0.2	b	2.3 ± 0.8

^a Error limits given only account for relative uncertainties. ^b Data quality does not allow reliable quantification.

**Figure 1.** Observed (symbols) and modeled (solid lines) ion abundances in the reactions of Pt_2CH_2^+ with D_2 .**Figure 2.** Observed (symbols) and modeled (solid lines) ion abundances in the reactions of Pt_3CH_2^+ with D_2 (and traces of background water).

quantitative treatment in the cases of $n = 4, 5$, the data for reaction 23a imply an enhanced reactivity of Pt_4CH_2^+ , which is in accordance with the findings presented above. In a closer analysis of the reactions of the smaller clusters Pt_nCH_2^+ ($n = 1-3$), statistics as well as the possible operation of kinetic isotope effects have to be considered. Yet, already the raw data suggest that PtCH_2^+ and Pt_2CH_2^+ essentially behave the same (Table 2). This is somewhat surprising, because the reactions with both NH_3 and H_2O clearly discriminate between these two platinum-carbene cations. In contrast, Pt_2CH_2^+ and Pt_3CH_2^+ (Figures 1 and 2) substantially differ in the rate constants determined for reaction 23c, although these clusters behave similarly in their reactions with NH_3 and H_2O .

For a quantitative evaluation, let us first assume complete equilibration of all four H/D atoms present in the collision complex. After compensation for statistical par-

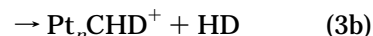
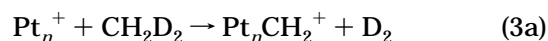
Table 3. Intramolecular Kinetic Isotope Effects (KIEs)^a of the Reactions of Pt_n^+ with CH_2D_2 (Reactions 3a–c)

	$n = 1$	$n = 2$	$n = 3$	$n = 4$	$n = 5$
KIE(3b/3a)	1.7 ± 0.2^b	1.2 ± 0.1	1.1 ± 0.2	1.3 ± 0.1	1.0 ± 0.1
KIE(3c/3b)	1.7 ± 0.1^b	1.2 ± 0.1	1.5 ± 0.1	1.3 ± 0.2	1.4 ± 0.2

^a Corrected for statistical effects; see text. ^b Compare with KIE(3b/3a) = KIE(3c/3b) = 1.6 reported in ref 23.

tituting (1:4:1 for losses of $\text{H}_2/\text{HD}/\text{D}_2$ from $[\text{Pt}_n\text{C}, \text{H}_2, \text{D}_2]^+$), one finds that the microscopic rate constant for reaction 23c is higher than that of reaction 23a by a factor of 1.8 ± 0.6 and 2.1 ± 0.9 for $n = 1, 2$, respectively. Two different explanations can be put forward in order to rationalize this result. Operation of KIEs is thought to favor elimination of H_2 (reaction 23c) compared to loss of HD (reaction 23a). Alternatively, the assumed complete equilibration of all H/D atoms might be invalid. If structures such as $\text{Pt}_n\text{C}(\text{H}_2)^+$ play an important role, direct exchange of the dihydrogen unit according to reaction 23c is thought to predominate. However, none of these arguments accounts for the deviating behavior of Pt_3CH_2^+ ; thus, its origin remains unclear.

An alternative approach for an investigation of the $[\text{Pt}_n\text{C}, \text{H}_2, \text{D}_2]^+$ systems starts from the reactions between Pt_n^+ and CH_2D_2 as different entrance channel (reactions 3a–c).



In contrast to reactions 23a–c, all four H/D atoms are a priori equivalent, such that differences in the reaction rates directly reflect the intramolecular KIEs. For their derivation, again, the statistical weights of the individual product channels have to be acknowledged (1:4:1 for reactions 3a–c). The observed KIEs do not strongly depend on cluster size n (Table 3). Moreover, they are all relatively small and, thus, suggest that hydrogen migrations are not involved in the rate-determining steps. In line with this conclusion, the potential-energy surface proposed by Zhang et al. for the system Pt^+/CH_4 assigns the highest barrier to elimination of H_2 from a $(\text{H}_2)\text{PtCH}_2^+$ structure;²⁵ an analogous situation may be assumed for the clusters. KIE(3c/3b) can also be compared with the ratio derived for reactions 23c and 23a, which yield the analogous products while starting from different reactants. For $n = 1, 2$, one finds agreement within the experimental uncertainties, which indeed indicates equilibration of

(25) Zhang, X.-G.; Liyanage, R.; Armentrout, P. B. *J. Am. Chem. Soc.* **2001**, *123*, 5563.

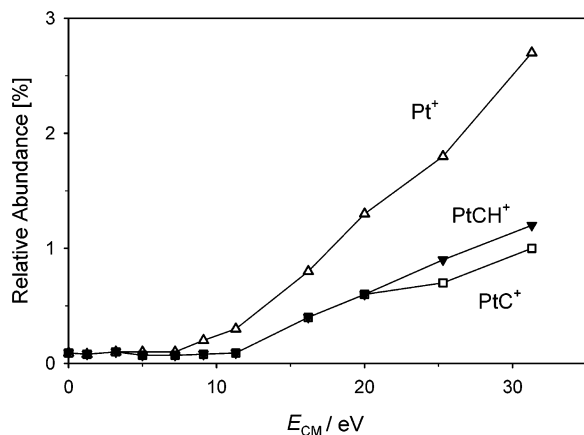
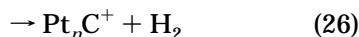
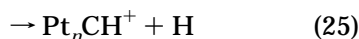
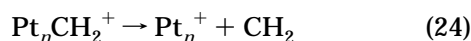


Figure 3. Relative abundances of the fragment ions in energy-dependent collision-induced dissociation (CID) of PtCH_2^+ .

all H/D atoms in the course of reaction 23. In contrast to the anomalous behavior observed in reaction 23 for $n = 3$, the KIE(3c/3b) value determined for this cluster size lacks any distinction.

(f) Collision-Induced Dissociation. A versatile means to probe the structures and energetics of gaseous ions are energy-resolved CID experiments. These monitor the dissociation of mass-selected ions as a function of collision energy. Ideally, the dissociation thresholds can be derived from the onsets of the corresponding fragments. Clearly, this approach requires the absence of multiple collisions, which would lead to ill-defined energy dependences. The validity of single-collision conditions can only be ensured if the pressure of the collision gas is kept low enough that the vast majority of the accelerated ions do not undergo any collision at all. In praxi, high signal-to-noise ratios are necessary to correctly determine the onset of fragmentation, as can be seen in the case of PtCH_2^+ (Figure 3). Here, for loss of CH_2 as the predominant CID process (reaction 24),



an apparent threshold between 5 and 10 eV (500 and 1000 kJ mol^{-1}) is observed when applying argon as collision gas. This value is roughly consistent with the apparent threshold between 5 and 6 eV reported by Zhang et al. using guided-ion beam mass spectrometry with xenon as collision gas and thus demonstrates the qualitative validity of the present energy-dependent CID experiments.²⁵ However, it is also obvious that the data quality does not allow a rigorous quantitative treatment; consequently, a more sophisticated analysis is not indicated. Yet, even at a semiquantitative level, interesting comparisons can be drawn. For instance, reaction 24 is apparently favored over the dissociations leading to PtCH^+ and PtC^+ (reactions 25 and 26 with $n = 1$), respectively. Because $D_0(\text{Pt}^+ - \text{CH}_2) = 463 \pm 3 \text{ kJ mol}^{-1}$ exceeds $\Delta_r H_0^\circ(25, n = 1) = 346 \pm 10$ and $\Delta_r H_0^\circ(26, n =$

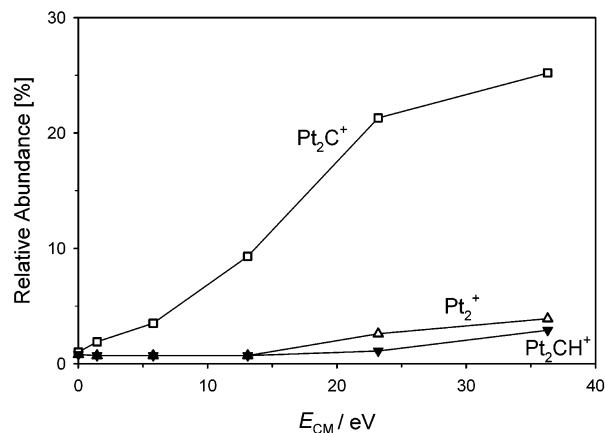


Figure 4. Relative abundances of the fragment ions in energy-dependent collision-induced dissociation (CID) of Pt_2CH_2^+ .

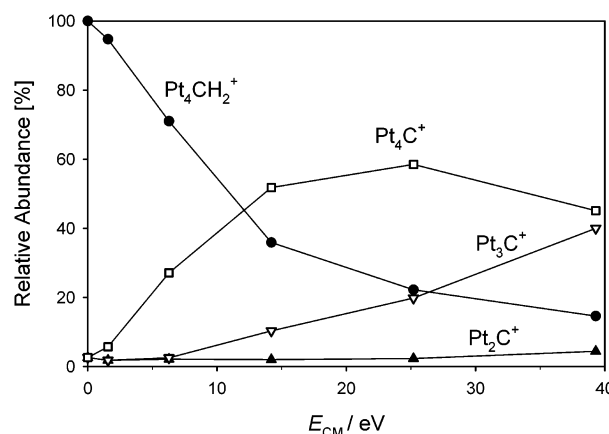
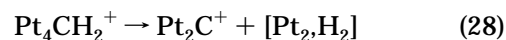
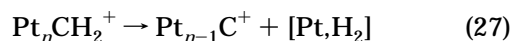


Figure 5. Relative abundances of the parent ion and its fragments in energy-dependent collision-induced dissociation (CID) of Pt_4CH_2^+ .

1) = $260 \pm 6 \text{ kJ mol}^{-1}$,^{25,26} considerable barriers seem to be associated with loss of H^\bullet or H_2 . In marked contrast, dehydrogenation according to reaction 26 predominates for $n = 2$ (Figure 4). The low appearance energy of this process, $\text{AE} \leq 1 \text{ eV}$, accounts for its relatively high efficiency, whereas occurrence of reactions 24 and 25 requires much larger collision energies and is much less effective.

For the larger clusters, carbide formation corresponding to reaction 26 gains even more in importance with appearance energies $\text{AE} < 2 \text{ eV}$. In the case of $n = 3$, the only other fragmentation observed is reaction 25, giving small amounts of Pt_3CH^+ . For Pt_4CH_2^+ and Pt_5CH_2^+ , this dissociation channel no longer occurs, whereas, in addition to simple dehydrogenation, one and (for $n = 4$) even two platinum atoms are lost at elevated collision energies (reactions 27 and 28, respectively)



(Figure 5). The finding that Pt_4CH_2^+ does only give platinum–carbide clusters Pt_4C^+ , Pt_3C^+ , and Pt_2C^+ but

(26) Lias, S. G.; Bartmess, J. E.; Liebman, J. F.; Holmes, J. L.; Levin, R. D.; Mallard, W. G. *J. Phys. Chem. Ref. Data Ser.* **1988**, *17*, Suppl. 1.

Table 4. Bimolecular Rate Constants k and Efficiencies φ for the Reactions of Pt_nC^+ with NH_3 , CH_4 , and O_2 , Respectively

reaction	eq no.	n	$k/cm^3 s^{-1}$	$\varphi = k/k_c^a$
$Pt_nC^+ + NH_3 \rightarrow [Pt_nC,H,N]^+ + H_2$	29	1	3.7×10^{-10}	0.18
$PtC^+ + NH_3 \rightarrow [Pt,C,H_2,N]^+ + H$	30		7.2×10^{-11}	0.036
$Pt_nC^+ + NH_3 \rightarrow [Pt_nC,H_3,N]^+$	32	3	$1.5 \times 10^{-11 b}$	8×10^{-3}
		4	$8.7 \times 10^{-11 b}$	0.044
		5	$1.7 \times 10^{-10 b}$	0.086
$Pt_nC^+ + CH_4 \rightarrow [Pt_nC_2,H_2]^+ + H_2$	35	1–4	$\leq 2 \times 10^{-12}$	$\leq 2 \times 10^{-3}$
		5	5.7×10^{-10}	0.60
$PtC^+ + O_2 \rightarrow Pt^+ + CO_2$	36		3.9×10^{-12}	7×10^{-3}
$Pt_nC^+ + O_2 \rightarrow Pt_nO^+ + CO$	37	1	6.7×10^{-12}	0.012
		2	$\leq 1 \times 10^{-13}$	$\leq 2 \times 10^{-4}$
		3	$\leq 5 \times 10^{-13}$	$\leq 1 \times 10^{-3}$
		4	1.6×10^{-10}	0.30
		5	2.8×10^{-10}	0.53
$PtC^+ + O_2 \rightarrow PtCO^+ + O$	38		3.4×10^{-12}	6×10^{-3}
$Pt_4C^+ + O_2 \rightarrow Pt_3C^+ + PtO_2$ (39)			4.2×10^{-11}	0.079

^a Collision rates k_c calculated according to capture theory (Su, T. J. *Chem. Phys.* **1988**, *89*, 4102, 5355). ^b Apparent bimolecular rate constant at $p(NH_3) \approx 3 \times 10^{-8}$ mbar presumably including termolecular contributions.

no bare Pt_4^+ upon CID demonstrates a strong binding of the carbide ligand to the cluster core. Most probably, this interaction involves more than a single metal center, which implies an even larger bond-dissociation energy than for the mononuclear carbide: $D_0(Pt^+-C) = 524 \pm 5$ kJ mol⁻¹.²⁵ Notably, the enhanced stabilities of the carbide clusters Pt_nC^+ can also account for the ready dehydrogenation of the carbene clusters $Pt_nCH_2^+$ in their reactions with NH_3 and H_2O (see above).

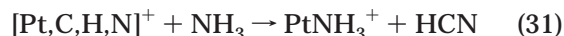
Pt_nC^+ . Because the experiments probing the reactions of platinum-carbene clusters $Pt_nCH_2^+$ could address the reactivity of platinum carbides Pt_nC^+ only indirectly, further efforts were undertaken to explicitly treat this issue. Unlike the situation for the carbenes, neither the behavior of the smallest carbide, PtC^+ , nor those of the homologous clusters have been investigated before. Pt_nC^+ ions can be generated by reaction of Pt_n^+ with CH_4 or C_3O_2 at elevated energies (see Experimental Section for details).

(a) Reactions with Ammonia and Water. The reactions observed for the system PtC^+/NH_3 are rather complex. As primary processes, both dehydrogenation (65% br) and loss of a single hydrogen atom (35% br) take place (reaction 29 with $n = 1$ and reaction 30)



(Table 4). Reaction 30 is remarkable because it involves the release of atomic hydrogen, which clearly is a highly energetic species. The occurrence of this process implies that PtC^+ must lie energetically high as well, resulting in enhanced reactivity and reduced selectivity. Concerning reaction 29, the most interesting question is whether this process mediates C–N bond coupling. CID, as a potential means to probe an ion's connectivity, is not considered a proper method in the present case because loss of HCN is expected to be the energetically most favorable fragmentation channel of $[Pt,C,H,N]^+$ regard-

less of its structure. Some more information can be gained from the consecutive reactions. The major secondary product NH_4^+ arises from both $[Pt,C,H,N]^+$ and $[Pt,C,H_2,N]^+$ by simple proton transfer, whereas the minor consecutive product $PtNH_3^+$ is attributed to ligand exchange of $[Pt,C,H,N]^+$ (reaction 31). Modeling



of the product distributions on the basis of this kinetic scheme reproduces the experimental data quite well.

Occurrence of reaction 31 suggests the presence of a preformed HCN (or CNH) unit in $[Pt,C,H,N]^+$. Thus, PtC^+ induces C–N bond formation upon reaction with NH_3 and resembles the carbene $PtCH_2^+$ in this respect. Apparently, PtC^+/NH_3 and $PtCH_2^+/NH_3$ are different entrance channels to the same potential-energy surface. The latter corresponds to a rather early step on the way toward HCN formation and stops after single dehydrogenation with the aminocarbene $PtC(H)NH_2^+$ as product (besides generation of $CH_2NH_2^+$). Further elimination of H_2 requires additional energy: i.e., CID of $PtC(H)NH_2^+$.¹³ In contrast, PtC^+/NH_3 enters the potential-energy surface at a later point, as loss of the first H_2 equivalent has already occurred in comparison with $PtCH_2^+/NH_3$. The energy gained from the interaction energy between NH_3 and PtC^+ is sufficient for dehydrogenation.

For the carbide derived from the platinum dimer, Pt_2C^+ , reaction 29 is the only primary process observed. Compared to $n = 1$, the lower efficiency of this reaction (Table 4) and also the absence of neutral open-shell products suggest Pt_2C^+ to be a significantly less energetic species than its smaller homologue. Nevertheless, its ability to activate NH_3 demonstrates a distinct reactivity of this species. Consideration of the consecutive reactions helps to elucidate the connectivity of the $[Pt_2,C,N,H]^+$ product. In contrast to its smaller analogue, $[Pt_2,C,N,H]^+$ does not undergo ligand exchange with NH_3 (reaction 31) but simply adds this substrate, probably assisted by termolecular stabilization. This process does not necessarily indicate the preformation of a HCN unit in $[Pt_2,C,N,H]^+$, because ligand exchange might be expected in that case. Moreover, protolysis reactions giving NH_4^+ only play a minor role in this system, whereas they predominate for the mononuclear homologue. As HCN bound to a metal cation is thought to exhibit an appreciable acidity, the low tendency of $[Pt_2,C,N,H]^+$ to transfer its proton does in fact dispute the presence of an HCN entity as well. However, if C–N coupling does not take place, the question arises as to which effect the carbide ligand has in NH_3 activation at all. Interestingly, bare Pt_2^+ was observed to even more readily dehydrogenate NH_3 .¹⁹ Although the strong binding of the carbon atom certainly significantly alters the electronic and geometric features of the cluster's metal core, the dehydrogenation observed might still reflect the intrinsic reactivity of the platinum dimer.

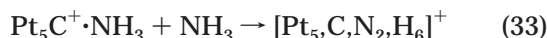
For the larger clusters, simple additions of NH_3 take place as primary processes (reaction 32 with $n = 3–5$).



The efficiency of this reaction is low for $n = 3$ but increases with cluster size (Table 4). Such a behavior

is well-known for association reactions in the highly diluted gas phase, where three-body collisions that could stabilize the collision complex between ion and substrate are unlikely but gain in importance for larger systems. Simple adduct formation leads to $Pt_nC^+ \cdot NH_3$ structures: i.e., those inferred for the products of the reactions between $Pt_nCH_2^+$ and NH_3 (reaction 6). Similar to the couple $PtCH_2^+$ and PtC^+ , the reactions of NH_3 with the platinum–carbene and –carbide clusters access the same potential-energy surfaces. Accordingly, $Pt_nC^+ \cdot NH_3$ adds further NH_3 (reaction 8), regardless of its origin from $Pt_nCH_2^+$ or Pt_nC^+ .

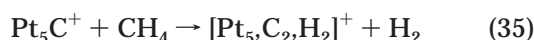
The reactivities of Pt_nC^+ ($n = 3–5$) toward ammonia may also be compared with those of the bare platinum clusters Pt_n^+ (see above for $n = 2$). In analogy to reaction 32, the Pt_n^+ clusters ($n = 3–5$) simply add NH_3 .¹⁹ Hence, the carbide ligand acts as an adatom, which only constitutes a minor perturbation with respect to the reactivity of the cluster core. Remarkable features of the bare clusters Pt_4^+ and particularly Pt_5^+ are the N–H bond activations observed in consecutive reactions with NH_3 . The fact that dehydrogenation only occurs after addition of at least two NH_3 ligands was rationalized by elimination of H_2 stemming from two different NH_3 entities.¹⁹ Notably, the same behavior is observed for $Pt_5C^+ \cdot NH_3$: reaction with NH_3 yields $[Pt_5, C, N_2, H_6]^+$ and $[Pt_5, C, N_2, H_4]^+$ (reactions 33 (70% br) and 34 (30% br)).



Apparently, the reactivities of the platinum–carbide clusters toward NH_3 indeed resemble those of Pt_n^+ .

In contrast to the diverse reactivity of Pt_nC^+ clusters toward NH_3 , no reactions at all were observed with water. Again, this difference is attributed to the lower nucleophilicity of H_2O , which also manifests itself in the extremely low reaction rates for the formation of adducts with bare Pt_n^+ clusters.¹⁹

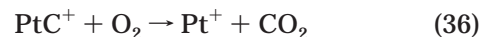
(b) Reactions with Methane. The parallels between the reactivities of Pt_n^+ and Pt_nC^+ clusters entirely disappear in the case of CH_4 , however. Whereas carbene formation occurs for all bare Pt_n^+ clusters,^{18,19} only Pt_5C^+ is able to dehydrogenate methane (reaction 35).



This situation clearly resembles that observed for $Pt_nCH_2^+$, where also all clusters except the pentamer failed to activate CH_4 . In contrast to its carbide counterpart, however, the carbene derived from atomic platinum effects slow dehydrogenation of CH_4 . Presumably, this difference arises from the distinct bond orders in $PtCH_2^+$ and PtC^+ . Whereas the carbene exhibits a double bond, the binding in the carbide rather corresponds to a triple bond.²⁵ Thus, in PtC^+ the valencies of the metal center are thought to be more saturated, which would account for the decreased reactivity toward CH_4 .

(c) Reactions with Dioxygen. Finally, the reactions of platinum–carbide clusters with O_2 were investigated.

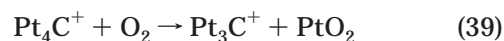
For mononuclear PtC^+ , three different processes occur (reactions 36–38 with $n = 1$).



Reactions 36 (28% br) and 37 (48% br) are oxidation processes that meet expectations. Quite surprising is the occurrence of reaction 38 (24% br), in which atomic oxygen is released. To render the overall process exergonic, the reactants are supposed to provide considerable amounts of energy. Thus, again, a relatively low stability of PtC^+ is implied. Of course, formation of the extremely stable C–O bond shifts the energy balance in favor of the products as well. The binding between the metal and the CO ligand as a whole also significantly contributes to the achieved total exoergicity ($D_0(Pt^+ - CO) = 212 \pm 10 \text{ kJ mol}^{-1}$).²⁷

In contrast, Pt_2C^+ and Pt_3C^+ do not react with O_2 . For Pt_4C^+ and Pt_5C^+ , however, oxidation according to reaction 37 occurs quite efficiently, whereas losses of neutral CO_2 or O do not take place. Absence of the latter channel is in line with an increased stability of the platinum–carbide clusters compared to PtC^+ . With respect to the tradeoff between production of CO and CO_2 , the former already prevails for atomic platinum; enlargement of the metal core is thought to increase its oxophilicity and, thus, to further favor CO formation, in agreement with experiment.

In comparison to the reactions between $Pt_nCH_2^+$ and O_2 , oxidation of the carbides does not stop at the bare platinum clusters but proceeds until Pt_nO^+ , which simply reflects the availability of two reduction equivalents less than in the case of the carbenes. Besides formation of CO, O_2 also induces degradation of Pt_4C^+ the cluster (reaction 39; 20% br). This type of reactivity



corresponds to that known for Pt_n^+ and, again, indicates similarities between the carbide and the bare platinum clusters.¹⁹

Conclusions

The reactions of platinum–carbene clusters $Pt_nCH_2^+$ with the nucleophilic substrates NH_3 and H_2O reveal pronounced differences between the reactivities of $PtCH_2^+$ and the corresponding clusters $Pt_nCH_2^+$. Whereas atomic platinum mediates carbon–heteroatom bond coupling and thereby accomplishes methane functionalization, the homologous clusters fail in this respect and lead to formation of carbide structures instead. Reactivity studies of independently generated Pt_nC^+ clusters fully support this conclusion. While one possible rationalization for the distinct behavior of the clusters relies upon different ion structures, analysis of KIEs and H/D exchange processes does not reveal significant differences between $PtCH_2^+$ and the corresponding clusters, as one would expect for distinct structures. Because

(27) Zhang, X.-G., Armentrout, P. B. *Organometallics* **2001**, *20*, 4266.

hydrogen rearrangements appear to be facile for all Pt_nCH_2^+ species studied, the structural argument further loses relevance, particularly if one takes into account that the strong interactions between the ion and the nucleophilic reagents provide considerable amounts of energy for surpassing any barriers associated with such processes. A second conceivable explanation refers to energetic differences of the product channels. Absence of carbide formation in the reactions of PtCH_2^+ with NH_3 and H_2O , respectively, suggests a thermochemical hindrance, because simple dehydrogenation resulting in carbide structures should be kinetically favored compared to entropically demanding carbon–heteroatom coupling. Indeed, the CID experiments prove the carbide clusters Pt_nC^+ to bind the carbon atom more strongly than their smaller homologue PtC^+ , which corroborates the energetical arguments. Most likely, the enhanced stability of the carbide clusters arises from the interaction of the carbon atom with more than a single metal center. Apparently, cationic platinum clusters resemble metal surfaces where soot formation is well-known to cause catalyst deactivation.²⁸

The reactions of cationic platinum carbenes and carbides with O_2 provide an alternative route for methane conversion. C–O bond coupling occurs for all cluster sizes except $n = 2$, which reflects platinum's high catalytic activity in oxidation processes. As a downside of this enhanced reactivity, the reaction does not stop at the stage of methanol but proceeds further to formation of CO or related compounds. Thus, the interaction of O_2 with platinum–carbene clusters results in over-oxidation, whereas no C–O coupling is achieved upon reaction with H_2O . As in bulk-phase chemistry, methane functionalization in the gas phase appears to require a delicate balance between the activity and selectivity of the catalytic system.

Experimental Section

Experiments were performed using a Spectrospin CMS 47X FT-ICR mass spectrometer which has been described in detail before.^{29,30} Recently,³¹ the instrument has been equipped with a Smalley-type³² cluster-ion source developed by Bondybey, Niedner-Schatteburg, and co-workers.³³ All experiments start with generation of Pt_n^+ clusters that are then subjected to different sequences of MS^n experiments.

Briefly, the fundamental of a pulsed Nd:YAG laser ($\lambda = 1064$ nm, Spectron Systems) is focused onto a rotating platinum target. The metal plasma thereby generated is entrained in a synchronized helium pulse and cooled by supersonic expansion so that cluster formation occurs. After passing a skimmer, a system of electrostatic potentials and lenses transfers the ionic components of the molecular beam into the analyzer cell, where they are trapped in the field of a 7.05 T superconducting magnet. The distribution of cluster ions can be somewhat controlled by varying the delays between helium pulse, laser

shot, and inlet into the analyzer cell. However, the best signal-to-noise ratios achieved for the clusters are still about 1 order of magnitude smaller than those of the Pt^+ monomer. For the larger clusters, the situation is particularly unfavorable, because the intensity is spread over broad isotopic distributions. To ensure an unambiguous product analysis, which is particularly important for the labeling studies, the formal $^{195}\text{Pt}_n^+$ isotopomers³⁴ were isolated by use of the FERETS technique.³⁵ The ejection of the neighbored isotopomers ($\Delta m/z = 1$) in the isolation procedure inevitably leads to a certain off-resonance excitation of the $^{195}\text{Pt}_n^+$ ions themselves. This kinetic excitation is easily probed by reaction with CH_4 ; whereas thermalized Pt_n^+ clusters ($n = 2-5$) solely effect single dehydrogenation of CH_4 (reaction 3), mainly 2-fold dehydrogenation leading to the carbide clusters Pt_nC^+ is observed after application of the FERETS isolation procedure. Occurrence of this endothermic process implies the availability of excess energy. In contrast, only Pt_nCH_2^+ clusters are formed if the mass-selected Pt_n^+ clusters are thermalized by collisions with pulsed-in argon buffer gas prior to reaction with CH_4 . Thus, simply the order of pulsing in Ar buffer gas and reactant CH_4 controls whether Pt_nCH_2^+ or Pt_nC^+ clusters are formed (in the case of deliberate generation of Pt_nC^+ , remaining Pt_nCH_2^+ is removed by resonant ion ejection prior to thermalization). Thermalization was assumed to be complete when the reaction rates did no longer depend on the number of argon pulses applied (typically, one or two pulses reaching a pressure of ca. 10^{-5} mbar for about 0.5 s were sufficient). In the case of PtC^+ , generation of this species by reaction of kinetically excited Pt^+ with CH_4 proved inefficient. Instead, reaction of Pt^+ with carbon suboxide, C_3O_2 ,³⁶ inter alia, gives PtC_2O^+ , which after mass selection yields PtC^+ upon CID. Thermalization of PtC^+ , like that of mass-selected Pt_n^+ clusters (required for determination of the KIEs associated with reaction 3), again was accomplished by pulsing in Ar buffer gas.

Ion–molecule reactions were studied by leaking in the neutral reactant at $p \approx (5 \times 10^{-9})-10^{-6}$ mbar and recording the decline of the reactant clusters and the evolution of corresponding products. Kinetic analyses yielding bimolecular rate constants k were derived on the basis of the pseudo-first-order kinetic approximation. The error of the rate constants reported is estimated at $\pm 30\%$ ³⁷ in general and $\pm 50\%$ for reactions with NH_3 and H_2O because of their unfavorable pumping characteristics. Consecutive reactions were analyzed using numerical routines.^{38,39} Particularly for the larger clusters studied, extensive data accumulation (up to 1000 scans) was necessary for achieving reasonable signal-to-noise ratios.

For CID, the mass-selected ions were accelerated to higher orbits by resonant excitation and collided with argon as buffer gas. The ion-cyclotron energy E_c was varied by changing the excitation time t_{exc} according to

$$E_c = \frac{\beta^2 e^2 V_{\text{pp}}^2 t_{\text{exc}}^2}{128 R^2 m} \quad (40)$$

with the geometrical factor of the ICR cell $\beta = 0.83$, the elementary charge e , the peak-to-peak voltage of the excitation

(28) Forzatti, P.; Lietti, L. *Catal. Today* **1999**, *52*, 165.

(29) Eller, K.; Schwarz, H. *Int. J. Mass Spectrom. Ion Processes* **1989**, *93*, 243.

(30) Eller, K.; Zummack, W.; Schwarz, H. *J. Am. Chem. Soc.* **1990**, *112*, 621.

(31) Engeser, M.; Weiske, T.; Schröder, D.; Schwarz, H. *J. Phys. Chem. A* **2003**, *107*, 2855.

(32) Maruyama, S.; Anderson, L. R.; Smalley, R. E. *Rev. Sci. Instrum.* **1990**, *61*, 3686.

(33) Berg, C.; Schindler, T.; Kantlehner, M.; Niedner-Schatteburg, G.; Bondybey, V. E. *Chem. Phys.* **2000**, *262*, 143.

(34) Note that the mass-selected $^{195}\text{Pt}_n^+$ clusters overlap with other isotopomers according to their natural abundances. Mass-selected Pt_2^+ with m/z 390, for example, corresponds to a mixture mostly containing $^{195}\text{Pt}_2^+$ and $^{194}\text{Pt}^{196}\text{Pt}^+$ along with a trace of $^{192}\text{Pt}^{198}\text{Pt}^+$.

(35) Forbes, R. A.; Laukien, F. H.; Wronka, J. *Int. J. Mass Spectrom. Ion Processes* **1988**, *83*, 23.

(36) C_3O_2 was prepared by dehydration of malonic acid; see: Beyer, H.; Walter, W. *Lehrbuch der Organischen Chemie*, 22th ed.; Hirzel: Stuttgart, Germany, 1991.

plates $V_{pp} = 8.4$ V, the radius of the cell $R = 0.03$ m, and the ion's mass m .⁴⁰ Conversion of the collision energy from the laboratory to the center-of-mass frame follows eq 41.

$$E_{CM} = \frac{m_{Ar}}{m_{Ar} + m} E_{lab} \quad (41)$$

(37) Schröder, D.; Schwarz, H.; Clemmer, D. E.; Chen, Y.-M.; Armentrout, P. B.; Baranov, V. I.; Böhme, D. K. *Int. J. Mass Spectrom. Ion Processes* **1997**, *161*, 175.

(38) Mazurek, U.; Schwarz, H. ICR Kinetics, version 3.0.1, Technische Universität Berlin, 1998.

(39) Mazurek, U. Dissertation, TU Berlin, D83, 2002.

(40) Sievers, H. L.; Grützmacher, H.-F.; Caravatti, P. *Int. J. Mass Spectrom. Ion Processes* **1996**, *157/158*, 233.

Acknowledgment. This work was funded by the Deutsche Forschungsgemeinschaft and the Fonds der Chemischen Industrie. Further, we acknowledge Degussa AG for generous support. K.K. particularly thanks the Stiftung Stipendien-Fonds des Verbandes der Chemischen Industrie for a Kekulé scholarship.

OM030272L